

Accurate Models of NVIDIA Tensor Cores

Faizan A. Khattak and Mantas Mikaitis

School of Computer Science, University of Leeds, Leeds, UK

Abstract—Matrix multiplication is a fundamental operation in both training of neural networks and inference. To accelerate matrix multiplication, Graphical Processing Units (GPUs) provide it implemented in hardware. Due to the increased throughput over the software-based matrix multiplication, the multipliers are increasingly used outside of AI, to accelerate various applications in scientific computing. However, matrix multipliers targeted at AI are at present not compliant with IEEE 754 floating-point arithmetic behaviour, with different vendors offering different numerical features. This leads to non-reproducible results across different generations of GPU architectures, at the matrix multiply-accumulate instruction level. To study numerical characteristics of matrix multipliers—such as rounding behaviour, accumulator width, normalization points, extra carry bits, and others—test vectors are typically constructed. Yet, these vectors may or may not distinguish between different hardware models, and due to limited hardware availability, their reliability across many different platforms remains largely untested.

We present software models for emulating the inner product behavior of low- and mixed-precision matrix multipliers in the V100, A100, H100 and B200 data center GPUs in most supported input formats of interest to mixed-precision algorithm developers: 8-, 16-, and 19-bit floating point. These matrix multiplier models are first approximated by determining the numerical features via test vectors designed to trigger outputs sensitive to bit level differences in the implementation, followed by semi-exhaustive comparison (randomised input vectors of 10^5 values) between the models and the actual GPU matrix multipliers—this process is repeated until the model is bit-accurate. These models enable verification of test vectors before applying them to real hardware and also support computational scientists and mixed-precision algorithm developers with easy-to-use accurate models available in MATLAB—we demonstrate their use in multi-word emulation algorithms for matrix multiplication.

The software associated with this paper, the MATLAB Tensor Core v0.1, which includes various NVIDIA GPU tensor core models as well as a generalised model that can be used to instantiate custom tensor core variants, is available on GitHub: <https://github.com/north-numerical-computing/MATLAB-tensor-core>.

I. INTRODUCTION

Most recent GPUs incorporate specialized matrix multiplier units, often referred to as *tensor cores* or *matrix engines*, which are designed to accelerate general matrix multiply operation (GEMM) for AI workloads. Beyond neural networks, these units are also extensively used to accelerate fundamental linear algebra kernels used in high-performance computing (HPC) applications outside of AI [1], [2], [3]. Almost half of the machines on the November 2025 TOP500 list¹ contain low-

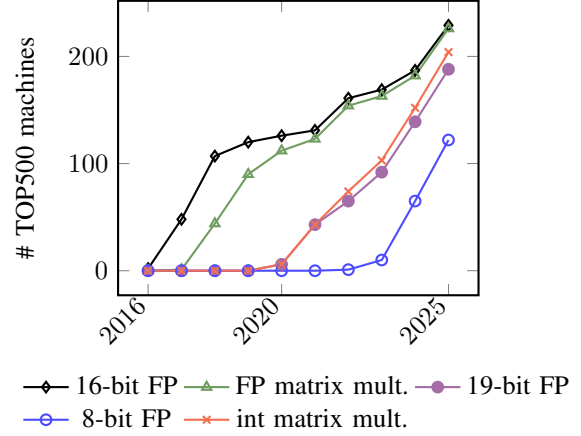


Fig. 1. Number of machines on the November TOP500 lists that support low-precision floating-point formats, and low- and mixed-precision matrix multiplication operations. NVIDIA, AMD, and Intel GPUs are included in the counts.

precision matrix multiplication operation in hardware and there is no sign of the slowing growth (Fig. 1).

Support for very low-precision, 8-, 6-, and even 4-bit, floating-point formats (albeit with higher precision accumulation in the inner products) is widely available in AMD [4] and NVIDIA [5] GPU architectures. In this paper we will focus on NVIDIA matrix multipliers, informally known as *tensor cores*. Tensor cores generally do not adhere to any numerical standards, likely due to the absence of mixed-precision arithmetic standards at the time of their introduction in the NVIDIA V100 GPU in 2017. Until the establishment of relatively recent Open Compute Project [6] and IEEE P3109 [7] standardisation activities, there was no standard for low-precision number formats and arithmetic. Consequently, even today, AI hardware vendors implement mixed-precision matrix multipliers in various ways, and the computed matrix products across architectures and vendors may differ. While some of the latest hardware implements the OCP data formats [6], the OCP does not standardise arithmetic behaviour.

Mixed-precision tensor cores also do not follow the IEEE 754 [8] behaviour, because that would require relatively expensive normalisation and rounding logic to be evaluated on every FMA operation within the matrix multiply unit, which may not be justified for AI workloads that may tolerate rounding errors. The features of interest (that cause most impact to the matrix products) include normalization points in multi-term floating-point addition, the adopted rounding modes, the block fused multiply-accumulate (FMA) size (number of

¹<https://top500.org/lists/top500/list/2025/11/>

additions in a dot-product-add operation), and the use of extra bits in intermediate alignments of significands of products, amongst others. The lack of standardization across vendors makes reproducibility and explainability of numerical results particularly challenging in scientific computing applications which may rely on cross-platform consistency. It can also cause difficulties for performing accurate error analysis of algorithms that utilise mixed-precision matrix multipliers.

A. Previous work

The numerical characteristics of mixed-precision matrix multipliers are seldom documented. Nonetheless, recent studies have attempted to characterize some of these features using input vectors, compiled manually or through theorem provers, that trigger special cases in the matrix multipliers of different designs to produce unique results, allowing one to reason about the overall numerical behaviour without checking all the possible inputs. Such studies have been done for AMD, Intel, and NVIDIA GPUs [9], [10], [11], [12], [13]. These works have developed conceptual models of matrix multipliers in different generations of NVIDIA tensor cores, but we argue, using randomised testing of tensor cores and their models, that refinement is needed to improve their accuracy. The aim of this project is to provide an accurate model of a tensor core in MATLAB, to enable the mixed-precision research community to perform accurate numerical experiments with the algorithms that target tensor cores. Therefore to more accurately simulate the behavior of tensor cores, we develop an iterative technique that allows us to refine the models.

This type of work goes back to the *Paranoia*² software, built in the 1980s, for testing the compliance with the IEEE 754 standard. Several projects followed. Hillesland and Lastra [14] developed a GPU Paranoia which allowed them to analyse R300 and NV30 devices and found that, for example, basic arithmetic operations were not optimally accurate as prescribed by the *correct rounding* of IEEE 754. The FPGA Paranoia of Tan, Boland, and Constantinides [15] similarly tested the arithmetic of various FPGA devices, finding for example that Altera devices rounded division differently from Xilinx devices, by not rounding to the nearest number in some cases.

B. Contributions

In this work, we reapply the generalized test vectors proposed in our earlier study [13] to determine the numerical features of NVIDIA's V100, A2, A30, A100, H100, H200, L40S, Ada RTX 1000, and B200 tensor cores across all supported input and output precisions. Unlike prior analyses in [9], [10], [11], [12], [13], we extend the investigation to include the two 8-bit floating-point formats available on the L40S, Ada RTX 1000, H100, H200, and B200 GPUs. Based on the identified features, we develop MATLAB-based software models of tensor cores for the aforementioned GPUs, for increasing the productivity and accessibility to tensor

cores by mixed-precision algorithm developers and numerical analysts. Features that we cannot find initially are identified by comparing the outputs of the emulated models against actual GPU results, and subsequently verified using targeted test vectors. This iterative approach aims to refine the MATLAB models to an acceptable level of accuracy.

In addition, our MATLAB toolbox provides a customizable tensor core model that allows users to diverge from one of the GPU tensor core models by customizing the precision and rounding behaviour. The models are developed by combining fixed-point arithmetic with the custom floating-point format simulator CPFloat [16].

We demonstrate the use of the models on two example applications:

- numerical feature test vector authentication, and
- emulation of high-precision matrix multiplication on tensor cores [17], [18], [19], [20].

The main contributions of this paper are summarized as follows:

- Determination of various numerical features for NVIDIA V100, A100, A2, A30, H100, H200, B200, L40S, and RTX 1000 Ada tensor core models, including 8-bit floating-point formats. We have presented these features more precisely than any other previous work, using architectural diagrams.
- Development of MATLAB-based simulation models for GPU tensor cores, validated against GPU results through randomised matrix multiplication input space coverage.
- We provide experimental results on the differences that tensor cores can cause in a low-level kernel, multi-word matrix multiplication, which serves as an example of how these models can be used by the community.

II. NOTATIONS AND DEFINITIONS

Table I shows some of the characteristics of various floating-point formats available on the latest NVIDIA Blackwell architecture. Hereafter we refer to floating-point formats with the following short-hand names: fp8 (either of fp8-E4M3 or fp8-E5M2), fp16 (binary16 IEEE 754), bf16 (bfloat16), tf19 (TensorFloat32), fp32 (binary32 IEEE 754), and fp64 (binary64 IEEE 754).

Take two matrices $A \in \mathbb{R}^{m \times k}$, $B \in \mathbb{R}^{k \times n}$. The matrix multiply-accumulate (MMA) operation produces

$$D = AB + C \in \mathbb{R}^{m \times n}.$$

Denote with d_{ij} the element at i th row and j th column of D . We can express it as the inner product between the i th row of A and j th column of B as

$$d_{ij} = \sum_{\ell=1}^k a_{i\ell} b_{\ell j} + c_{ij}.$$

²https://www.arithmazium.org/paranoia/aaapara_toc.html

TABLE I
FLOATING-POINT FORMATS THAT ARE AVAILABLE ON THE LATEST NVIDIA BLACKWELL GPUS [5]. PRECISION OF THE SIGNIFICAND, WHICH INCLUDES AN IMPLICIT BIT [8], MINIMUM REPRESENTABLE POSITIVE NORMALISED VALUE, AND MAXIMUM REPRESENTABLE POSITIVE VALUE, ARE SHOWN FOR EACH FORMAT.

| Format | precision | min norm. pos. | max pos. |
|-------------------|-----------|----------------|------------------------------|
| binary64 (double) | 53 | 2^{-1022} | $\sim 1.798 \times 10^{308}$ |
| binary32 (single) | 24 | 2^{-126} | $\sim 3.403 \times 10^{38}$ |
| tf32 (19-bit) | 11 | 2^{-126} | $\sim 3.401 \times 10^{38}$ |
| bf16 | 8 | 2^{-126} | $\sim 3.389 \times 10^{38}$ |
| binary16 (half) | 11 | 2^{-14} | 65504 |
| fp8-E4M3 | 4 | 2^{-6} | 448 |
| fp8-E5M2 | 3 | 2^{-14} | 57344 |
| fp6-E2M3 | 4 | 2^0 | 7.5 |
| fp6-E3M2 | 3 | 2^{-2} | 28 |
| fp4-E2M1 | 2 | 2^0 | 6 |

To focus on the inner product as an underlying operation, rather than on particular elements of D , we drop the subscripts for simplicity, and we have

$$d = \sum_{\ell=1}^k a_{\ell} b_{\ell} + c = \sum_{\ell=1}^k p_{\ell} + c. \quad (1)$$

The operations of the type (1) are often approximated in hardware by employing a multi-term floating-point adder [21]. In such adders, the significands of addends are aligned relative to the largest exponent either in a single global alignment or combination of local and global alignment steps [22], [23], and then subsequently added via a compressor or a tree of adders with a single rounding and normalisation step. For such many-term dot products, we define the number of product terms p_{ℓ} added in one go as the size of the *block fused multiply-accumulate*, following the naming convention used in the rounding error analysis of tensor cores by Blanchard et al [24], denoted with N_{FMA} . For instance, the tensor core in the A100 data center GPU has an FMA size of 8 for fp16 inputs which means $p_1 + \dots + p_8 + c$ is computed with a single normalisation and rounding. When such units perform multi-term significand alignment, the bits of each significand that are shifted to the right are truncated or rounded with multiple sticky bits [25]. In the alignment of significands, we denote the number of extra alignment or guard bits beyond the output precision by n_{eab} , similar to our previous work [13]. For instance, it has been shown by several studies that V100 GPU tensor core performs accumulation in 24 bits (the precision of the fp32 format), hence with $n_{\text{eab}} = 0$ [9], [10], [11].

III. METHODS

A. Generalised Numerical Feature Testing (GNFT)

This method for determining numerical features operates on the principle of using carefully designed expressions for forming test vectors that can trigger bit-level differences in the outputs [13]. For example, consider a test vector designed to determine whether subnormal inputs are supported in the fp16 format [8]. A test vector can be constructed by using

constants: $|a_1| < 2^{-14}$ (smallest normalised value in fp16; see Table I), $b_1 = 1$, and $a_{\ell} = b_{\ell} = 0$ for $\ell = 2, \dots, k$. This can be generalised for any format, by using an expression for the smallest normalised value.

When applying this test vector to a tensor core, if the resulting output d is non-zero, it indicates that subnormal inputs are supported (an outcome that has to be formulated by understanding the IEEE 754 floating-point arithmetic). Similarly, $a_1 = 2^{-14}$ and $b_1 = 2^{-1}$ would demonstrate if subnormals can be produced by arithmetic operations from normalised values. Several such numerical feature-specific test vectors using constant values have been proposed in the literature [10], [11], [9]. A generalized formulation, which addresses the limitations of earlier approaches by avoiding manually deriving constants or rerunning a theorem prover that has no upper bound on the run time [12], for each format/device, has been explored by us [13]—we rely on that approach here to determine the numerical features of tensor cores in nine NVIDIA GPU variants and develop accurate models of them.

B. Input Space Search Method (ISSM)

Once the GNFT method has identified the numerical features, a conceptual or software-based model of the hardware matrix multiplier can be constructed to simulate its behavior. To achieve higher confidence in this model, in comparison to the GPU implementation, the ISSM method is invoked to look for input vectors to (1) for which the GPU results deviate from those produced by the conceptual or software model. Such discrepancies can then be analyzed to refine the model until the tests pass. When mismatches occur, a generalised test vector can be constructed to specifically detect and characterize such numerical features when analysing new hardware.

It is worth to note that the input space of (1) is generally large and only a small proportion of it can be checked. For example, for $k = 16$ and 8-bit floating-point as an input format, the input space pair $\{a, b\}$ has approximately $256^{32} \approx 10^{77}$ possible inputs. For this work we have chosen to sample a , b , and c from a standard normal distribution. The comparison between the software models and the GPU results is then performed over a moderately large subset of 10^5 randomly drawn inputs. For checking exceptional cases like subnormals, $\pm \text{Inf}$, we use a specific finite set of test vectors. In the future, one may explore different strategies for ISSM, and try to exploit, for example, Schryer’s [26] strategy for picking floating-point test inputs.

For each of the nine GPUs we have tested, some of them have up to five input formats: fp8 (both E4M3 and E5M2), fp16 (both fp16 and fp32 output mode), bf16, and tf19, requiring a separate verification for each. In total, we have verified 9 models of tensor cores, each with several input/output format combinations, giving in total 30 model verification runs with randomized input vectors (see Table II).

C. Matrix Multiplier Model Approximation and Refinement

The overall algorithm for determining an accurate model of a tensor core is shown in Algorithm 1.

Algorithm 1 Pseudocode for the approximation and refinement of matrix multiply models.

- 1: GNFT: apply generalised test vectors [13] \triangleright *Initial approximation of the matrix multiply model is determined.*
- 2: **while** True **do** \triangleright *Refine the approximation of the model*
- 3: ISSM: generate random test vectors
- 4: For each test vector, compute matrix multiply on GPU and on the model
- 5: **if** GPU and the model results mismatch **then**
- 6: Inspect failure cases and modify the model
- 7: **else**
- 8: Break \triangleright *The model is sufficiently accurate.*
- 9: **end if**
- 10: **end while**

The step that modifies the model causes the biggest challenge in automating the whole process, because it requires an expert to look into the mismatching outputs between the GPU and the model, and develop hypotheses about the features of the model that need to be changed to match the GPU output. A lot of the manual work is removed by using the generalised testing vector to get the first approximation of the model, which means that Algorithm 1 can significantly accelerate the determination of features of future tensor cores. However, the full automation of Algorithm 1 is an open problem which we leave for future research.

IV. RESULTS

A. Accurate GPU Matrix Multiplier Models

Numerical features of matrix multiplier units on AMD and NVIDIA have been determined upto a certain degree of accuracy [9], [10], [11], [12]. Focusing on the NVIDIA GPUs, we now argue that the previous work was essentially just the first step in Algorithm 1 (Line 1), and that the models that were previously determined are inaccurate and require further refinement.

1) *V100 Data Center GPU*: Mixed-precision matrix multiplication units, or tensor cores, were introduced in the NVIDIA Volta architecture, namely, the V100 device. The V100 tensor cores support only fp16 as the input format with fp16 or fp32 as the output format [27]. Xi et al. [11] claim that the FMA size cannot be determined when there are no extra alignment bits compared with the precision of the output format. Following [13] we denote this situation with $n_{\text{eab}} = 0$. However, using the FMA size detection algorithm proposed in [13], we were able to identify an FMA size of 4, which is valid for both cases of $n_{\text{eab}} = 0$ and $n_{\text{eab}} \neq 0$. In addition, when the significands are aligned, bits that fall outside the internal accumulator's precision are truncated rather than accumulated into multiple sticky bits as is done in the algorithm by Tenca [25]. Further tests on the

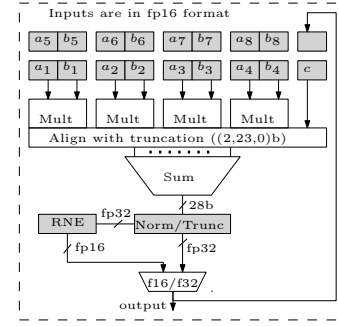


Fig. 2. A model of the inner product within the V100 GPU tensor core. Here, RNE denotes round-to-nearest-even rounding mode.

V100 GPU using this approach led us to the estimated tensor core model shown in Fig. 2, which differs from the model presented in [28, Fig. 2] in that the significand alignment is performed in 25 bits rather than 24, and c_1 is added together with the products rather than separately.

In our experiments, the existent conceptual model, when simulated in MATLAB, produced different results from the GPU for certain input combinations in the inner loop of Algorithm 1. Upon analysis, we determined that in some cases, partial products are not normalized before accumulation, which can result in variations even for apparently identical products. For instance, consider the case with $c = 0$, $p_1 = 2.25$, and $p_2 = p_3 = 2^{-23}$. Now consider two alternative ways to obtain the product $p_1 = 2.25$: either by assuming $a_1 = b_1 = 1.5$, or $a_1 = 1$, $b_1 = 2.25$. For the first case, the tensor core computed $d = 2.25 + 2^{-22}$, whereas for the second case, $d = 2.25$. In the first case, p_1 , which has the largest magnitude, is added in a denormalized form ($10.01_2 \times 2^0$), and hence p_2 and p_3 are not truncated. In contrast, in the second case, since $p_1 = 01.10_2 \times 2^1$, the remaining two products p_2 and p_3 fall outside the representable range (beyond the 23rd fractional bit), resulting in $d = 2.25$. On the other hand, if $c = 2.25$ with $p_1 = 0$, $p_2 = p_3 = 2^{-23}$, we have $d = c$. This feature is depicted in Fig. 2 as (2, 23, 0) bits at alignment stage where 2 represents integer bits, 23 fractional bits, and 0 the n_{eab} bits. It is worth noting that this test can be generalized, similar to our previous work [13] as it does not rely on the specific value such as 2.25; rather, any product greater than 2 and less than 4 can be used where the corresponding a and b have values $2 > a, b \geq \sqrt{2}$.

2) *A100 Data Center GPU*: In the fp32 output mode with fp16/bf16 as the input format, the FMA size is 8, and one extra bit is used internally, for the alignment and accumulation of significands of products p_ℓ . The rounding mode at both the alignment and post-normalization stages is truncation, whereas in fp16 output mode the rounding mode after normalization is Round-to-Nearest Ties-to-Even (RNE). The alignment of the significands is 26 bits wide, with 2 integer bits and 24 fractional bits, while the adder output must be

$$26 + \lceil \log_2(9) \rceil = 30 \text{ bits.}$$

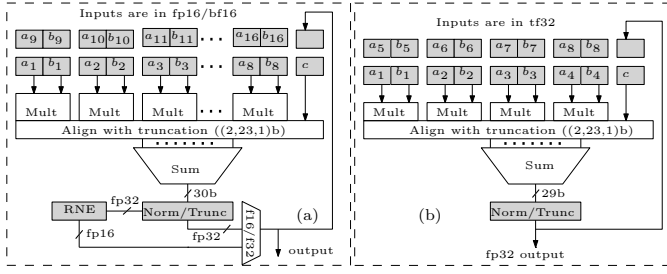


Fig. 3. A model of the inner product within the A100 GPU tensor core for the three input formats. A100 also has an fp64 tensor core, but that tensor core is compliant with the IEEE 754 FMA operation and is not shown here.

It should be noted that only three extra carry bits can be detected through testing [13], and although a fourth carry bit is assumed to exist by logic, to the best of our knowledge it cannot be verified through numerical tests unless we assume that there is no intermediate normalisation [12] when computing (1).³

The approximate model is shown in Fig. 3 (a). For tf19 input mode, the FMA size is reduced to 4, with truncation as the default rounding mode. The bit-width of the denormalised sum must be 29-bit wide. The model is shown in Fig. 3 (b). The products remain denormalised for fp16/bf16/tf19 input modes, as previously discussed in the context of V100. This behaviour can be verified by setting $c = 0$, $p_1 = 2.25$ where $a_1 = b_1 = 1.5$, and $p_2 = 2^{-23}$, $p_3 = p_4 = 2^{-24}$. When $d = 2.25 + 2^{-22}$, the products are added in denormalised form. The difference in this test compared to the V100 lies in the presence of an extra alignment bit ($n_{\text{eab}} = 1$) in the A100, which slightly alters the accumulation behaviour, making this test dependent on knowing the n_{eab} value.

In fp64 input/output mode, the FMA size is 1. This mode is compliant with IEEE 754 with RNE as the default rounding mode, but supports RD, RU and RZ. The observed accumulation order appears to follow

$$((c + p_1) + p_2) + \dots,$$

as indicated by permuting the values 1 , 2^{-53} , and 2^{-53} among c , p_1 , and p_2 . Only for the case $c = p_1 = 2^{-53}$ and $p_2 = 1$ does the GPU's tensor core produce $d = 1 + 2^{-52}$; for all other permutations, it returns $d = 1$ under the default RNE rounding mode. This behavior further suggests that the FP64 tensor core performs sequential FMA operations, where each intermediate result is fed back as the new input c .

3) *H100 Data Center GPU*: For fp16/bf16 input formats, the H100 tensor core is reported by Li et al. [11] to utilize two or more extra alignment bits, with fp32 as an output format, when the significands of the products are aligned for multi-term addition and summed. Using our generalised test vectors [13], we confirm that the H100 actually employs

³A test vector is needed, that can distinguish normalisation followed by the addition of the final addend, versus addition of the final addend to an accumulator that is in a denormalised form with the fourth carry bit set, followed by the final normalisation and truncation instead of rounding.

exactly $n_{\text{eab}} = 2$ extra alignment bits; no third alignment bit is present, and the bits of aligned significands that are out of range are truncated for fp16/bf16/tf19 input formats. As a result, the alignment module is 26-bits wide. However, since the products are added in denormalised form, same as in the V100 and A100 devices, the width of the significand alignment is $(2, 23, 2) = 27$ -bit wide, i.e., 2 integer, 23 fractional bits, and extra 2 bits of the fraction. This feature can be verified by setting $c = 0$, $p_1 = 2.25$, where $a_1 = b_1 = 1.5$, $p_2 = 2^{-23} + 2^{-24} + 2^{-25}$, and $p_3 = 2^{-25}$. If $d = 2.25 + 2^{-22}$, the largest product is kept denormalised, otherwise the output should be $d = 2.25$.

Furthermore, the FMA size is 16, which equals the maximum supported shared dimension of the matrix sizes available in the WMMA API. By the same reasoning, the denormalized adder result has a width of $27 + \lceil \log_2(17) \rceil = 32$ bits. Upon normalization, results are truncated rather than rounded. The fp16 format for both the input and output is supported, and the default rounding mode from the internal precision to the fp16 output is RNE. For the tf19 input mode, all numerical features are identical to those of the A100 model, except that two extra alignment bits are used instead of one. The fp64 input/output mode exhibits numerical features consistent with the fp64 tensor core of the A100.

The H100 and H200 GPUs also support two fp8 formats as the input format in the tensor cores, but the WMMA API does not provide direct support for those formats. Therefore, MMA instructions, which are PTX-level instructions, must be invoked directly. The matrix sizes supported by the MMA instruction for the fp8 input formats are

$$m \times n \times k = 16 \times 8 \times 16 \quad \text{and} \quad 16 \times 8 \times 32. \quad (2)$$

Here k denotes the shared dimension of the input A and B matrices supported by the tensor cores and can either be $k = 16$ or 32 . For both fp8 floating-point formats, fp8-E5M2 and fp8-E4M3, the output can be obtained either in fp16 or fp32 format.

- **fp32 output**: In this format, the inner product of two 32-element fp8 vectors is computed using two block FMAs of size 16. The first partial inner product s_1 is computed as

$$s_1 = \sum_{\ell} p_{\ell}, \quad \ell = 1, 2, 5, 6, 9, 10, \dots, 29, 30.$$

During this partial computation, two extra alignment bits beyond the 23 fractional bits are used, while the rest of the lower order bits are truncated. The accumulation then proceeds in single precision, with s_1 subsequently normalized and truncated to fp32. In this process, denormalized products during accumulation may occur, similar to the behavior observed for fp16, bf16, and tf19 input formats. For the second half of the inner product of 32 elements, the normalized and truncated s_1 is used as an addend in computing

$$s_2 = s_1 + \sum_{\ell} p_{\ell}, \quad \ell = 3, 4, 7, 8, 11, 12, \dots, 31, 32.$$

Here, the same features are present, except that alignment may be relative to s_1 if it is the largest operand, unlike in the first case where the input was zero and only the products were accumulated. Finally, the normalized and truncated result (in fp32) is added to c using the default round-to-nearest-even (RNE) rounding mode.

This interleaved pattern for computing the inner product of 32-element vectors can be verified by fixing $p_1 = 1$ and $p_2 = 2^{-24}$, and then assigning the value 2^{-24} sequentially to p_3 through p_{32} while keeping all other entries at zero. If $d = 1 + 2^{-23}$, the tested product falls into the same accumulation group as p_1 and p_2 . Conversely, if $d = 1$, the tested product belongs to the second group. If the two groups were not interleaved, we would observe $d = 1 + 2^{-23}$ only when assigning 2^{-24} to positions p_3 – p_{16} , and $d = 1$ when assigning it to positions p_{17} – p_{32} . For $k = 16$ case, we detected the same interleaved pattern.

- **fp16 output:** For fp16 outputs c and d , the internal accumulation still takes place in fp32 plus the extra alignment and carry bits. The first partial sum s_1 is normalized and rounded to fp16 using RNE. It is then used to compute s_2 in fp32 accumulation which is again normalized and reduced to fp16 precision with RNE. Finally, c is added to the reduced and normalized s_2 , with the final rounding mode set to RNE.

The FMA size detection algorithms presented previously [11], [13] are not directly applicable here, as they are constrained to the WMMA API. Furthermore, applying algorithms therein or test vectors directly, without modification, results in incorrect FMA size detection due to the overlapped nature of the halving of the 32-element vector into two parts. The best estimate of the tensor core model for the H100 GPU is illustrated in Fig. 4. It is also important to note that the fp8 model characteristics of the H100 GPU differ significantly from those of the Ada Lovelace RTX 1000 and NVIDIA L40S GPUs as discussed below.

The NVIDIA H200 GPU tensor cores exhibit numerical characteristics identical to those of the H100 (Fig. 4).

4) *B200 Data Center GPU Model:* B200 is the flagship data-centre GPU from NVIDIA, based on the Blackwell architecture, the latest iteration of the GPU architecture that is commercially available.

The B200 tensor cores, upon testing, reveal identical numerical behaviour to the H100/H200 models (Fig. 4). For single-precision accumulation with fp16/bf16 or tf19 inputs, the accumulator provides 2 extra bits, and the FMA tile sizes are 16/16 and 4, respectively. The fp8 tensor core also manifests the same interleaved inner-product partitioning of 32-element vectors as discussed previously for the H100/H200.

5) *L40S Data Center GPU Model:* Running the GNFT for fp16, bf16, and tf19 input formats, we determined that the L40S tensor cores exhibit behaviour identical to that of the A100, with FMA sizes of 8, 8, and 4, respectively, and with a single extra alignment bit when aligning significands, giving a 24-bit alignment/accumulation fraction in total. Bits that fall

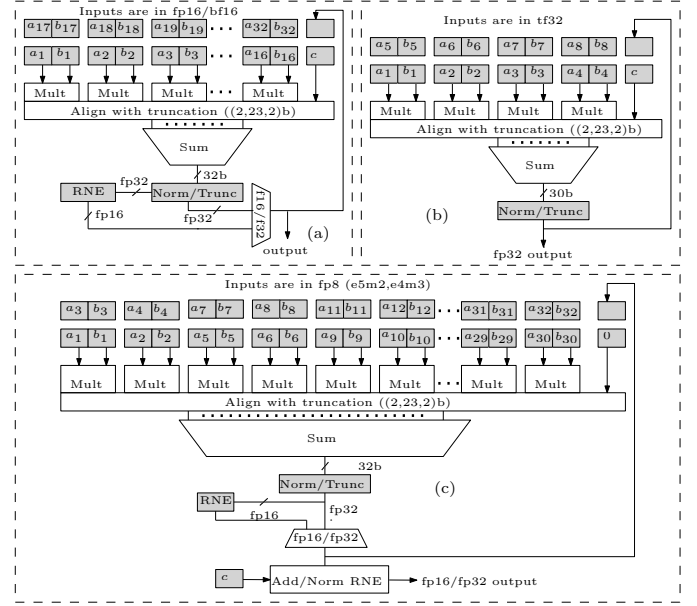


Fig. 4. A model of the inner product within the tensor cores of the H100/H200/B200 GPUs for (a) fp16/BF16, (b) tf19, and (c) fp8 input formats. The fp64 tensor core is compliant with IEEE 754 FMA operation and is not shown.

off the 24-bit fraction in the alignment of the significands during the multi-term floating-point addition are truncated, and the final results are truncated as well, unless the output is required in fp16 for the fp16 input setting. In this case, RNE is used as the default rounding mode.

When the input format is set to one of the fp8 formats, the interleaved pattern present for $k = 32$ in the H100/B200/H200 is not present in the L40S or RTX-1000 Ada (a consumer-grade GPU that we had available on a laptop and have also tested). For both fp8 formats, fp8-E5M2 and fp8-E4M3, the accumulation takes place with 13 fractional bits. We determined this by setting $p_1 = 1$, $p_2 = p_3 = 2^{-23-n_{eab}}$ and decrementing n_{eab} from 10 until d become equal to $1 + p_1 + p_2$. For $n_{eab} = -10$, we obtain $d = 1 + 2^{-12}$, which indicates that there are $23 - 10 = 13$ fractional bits, unlike the H100/H200/B200 where accumulation takes place within the 25-bit fraction. Moreover, we determined that c is added early with the first 16 products by setting $c = 1$ and $p_1 = p_2 = 2^{-14}$, which produced $d = 1$ in fp32 output mode.

The Ada Lovelace RTX 1000 consumer-grade GPU tensor cores exhibited identical numerical characteristics to those of the L40S model. This is further supported by the identical outputs produced by both models' tensor cores for inputs drawn from a single ensemble of 10^5 randomized input vectors. This is most likely because both GPUs belong to the Ada family and have fourth generation tensor cores on board. Since only the fp8 tensor core structure of the L40S is different compared with the tensor cores in the Ampere architecture (which does not accommodate fp8 at all), its best estimate is shown in Figure 5 only for the fp8.

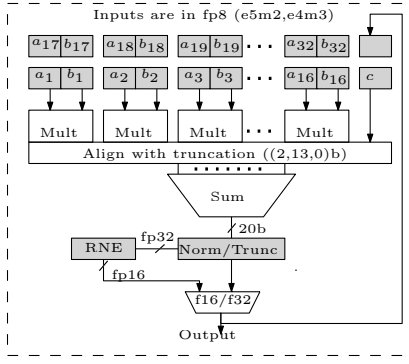


Fig. 5. A model of the inner product within the tensor cores of the L40S and Ada Lovelace RXT 1000 GPU for the fp8 input format.

6) *A2 & A30 Data Center GPUs*: Executing the GNFT on these GPUs and using the ISSM testing, we were able to determine that the tensor cores in these GPUs behave identically to the tensor cores of the A100 GPU, except that they don't support fp64 arithmetic in their tensor cores which the A100 does.

The numerical features of all nine GPU tensor cores are summarized in Table II, including the product alignment bits, accumulator output precision, N_{FMA} , final rounding mode to output precision, and other relevant details.

B. Authentication Via Randomized Testing

For accurate numerical analysis, reliable reproducibility, and consistent cross-platform comparison, the developed models must reproduce the exact results obtained from the corresponding hardware implementations. To verify this, outputs from the hardware and MATLAB-based models were compared over 10^5 randomized instantiations of $a = [a_0, \dots, a_k]$, $b = [b_0, \dots, b_k]$, and c , where all entries were drawn from a standard normal distribution. The tests were conducted across all supported input and output precision formats for all of the aforementioned NVIDIA devices.

For the hardware execution, the WMMA API was used for all supported data types except fp8, for which MMA instructions were invoked in CUDA. To further verify that tensor cores were active, the `cuobjdump` tool was used to inspect the compiled binary and confirm the presence of HMMA/QMMA/DMMA instructions. Across all tested configurations, the MATLAB models produced results that matched the hardware outputs exactly at the bit level for every run. It is important to note that this exact agreement was only achieved after properly incorporating the handling of denormalized products into the software models. A mismatch within the loop of Algorithm 1 was instrumental in revealing this feature and reiterating the validation. Furthermore, the interleaved pattern used in computing the inner products of input vectors on the H100/H200/B200 tensor cores was identified through a combination of discrepancies between software and hardware outputs for identical inputs and the results of the N_{FMA} determination algorithm in [13]. This algorithm produced

$N_{\text{FMA}} = 2$, indicating an interleaved pattern in the inner product computation; otherwise, N_{FMA} would not be smaller than $N_{\text{FMA}} = 16$ for fp16/bf16. In short, the refinement Algorithm 1 was executed for at least one iteration to find new features of tensor cores.

It is necessary to mention that the DMMA operations are not replicated or tested via randomized testing, nor are they included in the model package, as they behave as sequential FMAs and are fully IEEE compliant as reported by Fasi et al. [10]. Therefore, one can directly rely on MATLAB's built-in `fma` command to emulate the behaviour of DMMA.

Moreover, the emulated models are also designed to match the GPU outputs in exceptional cases (NaN, Inf, or -Inf), even though such values are not considered valid, meaningful, or desirable in mathematical or machine-learning computations. We have tested expressions such as $\infty \pm \infty$, $\pm(\text{Inf} \times \text{Inf})$, and $\text{NaN} \pm \text{Inf}$, both as direct inputs and as overflow scenarios where finite accumulations lead to $\pm \text{Inf}$ in the supported output formats. Consistent with GPU behavior, NaN takes precedence whenever it appears.

C. Example MATLAB Code for Using the Models

This section introduces the MATLAB Tensor Core v0.1. The toolbox was developed on MATLAB R2026a and depends on CPFloat [16]. Here we provide an insight into the user interface of this model, and briefly discuss some of the structure of the code.

The toolbox is comprised of three layers:

- `Generic_BFMA_TC.m`: provides a generalised tensor core model which can be set up with various features [13].
- `GEMM.m`: accepts α , A , B , β , and C , floating-point input and output formats, and the settings for the `Generic_BFMA_TC.m`, and approximates the GEMM $\alpha \times A \times B + \beta \times C$ using the tensor core model.
- A set of GPU tensor core models, such as `B200TC.m`, which instantiate the model parameters and call `GEMM.m`.

The v0.1 of the toolbox implements a recursive algorithm in `GEMM.m`, which is equivalent to recursively using a single tensor core to compute each inner product in the GEMM. It does not attempt to match the results of any CUDA GEMM implementations. Fig. 6 shows an example that calls the B200 tensor core model with an fp8 format as an input and fp32 as the output for multiplying two 4×4 matrices. Similarly, the user can call:

```
A100TC(alpha,A,B,beta,C,in_format,out_format)
V100TC(alpha,A,B,beta,C,out_format)
AdaTC(alpha,A,B,beta,C,in_format,out_format)
L40STC(alpha,A,B,beta,C,out_format)
```

H100 and H200 are identical to B200, and A2 is identical to A100 but can still be called as explicitly for completeness. Since V100TC supports fp16 input, only the output format type is required as input from the user. In addition, the user can call a custom model TC function with a set of parameters; an example is provided below.

TABLE II

SUMMARY OF THE NUMERICAL FEATURES OF SEVERAL GENERATIONS OF NVIDIA TENSOR CORES (MIXED-PRECISION MATRIX MULTIPLIERS) IN NINE DIFFERENT GPUS SPANNING YEARS OF RELEASE FROM 2017 TO 2024.

| Input | Output | GPU architectures | Prd. Align. Bitwidth | Acc. out. prec. | N_{FMA} | Final rounding | c ord. in acc. | Interleaved inputs |
|------------|--------|--------------------|----------------------|-----------------|------------------|----------------|------------------|--------------------|
| fp8 | fp32 | H100, H200, B200 | (2,25) | 32 | 16 | RNE | late | yes |
| | | L40S, Ada RTX 1000 | (2,13) | 20 | 16 | Trunc | early | no |
| fp8 | fp16 | H100, H200, B200 | (2,25) | 32 | 16 | RNE | late | yes |
| | | L40S, Ada RTX 1000 | (2,13) | 20 | 16 | RNE | early | no |
| fp16, bf16 | fp32 | H100, H200, B200 | (2,25) | 32 | 16 | Trunc | early | no |
| | | L40S, Ada RTX 1000 | (2,24) | 30 | 8 | Trunc | early | no |
| | | A100, A2, A30 | (2,24) | 30 | 8 | Trunc | early | no |
| | | V100 | (2,23) | 28 | 4 | Trunc | early | no |
| | | H100, H200, B200 | (2,25) | 30 | 4 | Trunc | early | no |
| tf19 | fp32 | L40S, Ada RTX 1000 | (2,24) | 29 | 4 | Trunc | early | no |
| | | A100, A2, A30 | (2,24) | 29 | 4 | Trunc | early | no |
| | | H100, H200, B200 | - | - | 1 | all 4 | early | - |
| fp64 | fp64 | A100 | - | - | 1 | all 4 | early | - |
| | | | - | - | 1 | all 4 | early | - |

Note: subnormal in/out supported; fp16 output for fp16 input is supported on all mentioned GPUs (rounded via RNE). The products remain denormalised in alignment and accumulation, reflected via 2 integer bits. Extra alignment bits n_{eab} are included in the fractional bits of the product alignment precision. Accumulation output precision is a sum of extra carry bits and the product alignment bits.

```
params.neab = 3; % extra alignment bits
params.fma = 32; % fma size
params.frmode = 'rne'; % final rounding mode
CustomTC(alpha,A,B,beta,C,...
    in_format,out_format,params)
```

A direct example of CustomTC model is provided in the form of B200TCRN which uses B200 features but with `params.frmode` set to `rne`. There is also a field `stkbitenab` in `params`, i.e., `params.stkbitenab`, which, when the significands of product terms are aligned, appends an extra sticky bit beyond the extra alignment bits, i.e., n_{eab} . By default, this is set to 0. In addition, the field `params.inter_pattern` is included due to the H100/H200/B200 tensor core behavior with the fp8 input format, discussed in Section IV-A3. If this field is set to 1, the custom model will compute the inner product of $2N_{\text{FMA}}$ -element vectors in two interleaved vectors, and the variable c is then added to the inner product at the end using a fixed RNE rounding mode (see Figure 4). The default value of this field is 0.

The `GEMM.m` file executes the parallelized version of matrix multiplication if the Parallel Computing Toolbox, introduced in MATLAB R2013b, is installed and the machine supports multicore processing. This ensures that computations are efficiently distributed across available CPU cores, accelerating large-scale matrix operations. If either is not supported, serialized version is executed.

V. NUMERICAL EXPERIMENTS AND APPLICATION EXAMPLES WITH THE TENSOR CORE MODELS

A. Numerical Features Test Vector Authentication

The tensor core models can be configured to replicate the numerical behavior of GPUs such as the V100, A100, and H100, or to use user-defined numerical features. Therefore, any test vector designed to target specific numerical properties

```
inopts.format = 'fp8-e4m3';
outopts.format = 'binary32';
A = cpfloat(randn(4), inopts);
B = cpfloat(randn(4), inopts);
C = cpfloat(randn(4), outopts);
B200TC(1,A,B,1,C, inopts.format, outopts.format)
```

```
>> ans =
    0.1484    -0.6631    -0.1836    -1.3271
    0.8232     1.6418     0.4805     3.0227
    3.6592    -0.1250     1.4902     2.2637
    3.7432    -3.4275     0.2031     0.1663
```

Fig. 6. An example MATLAB listing showing how to call the GEMM with the model of the tensor core from the NVIDIA B200 GPU.

can be verified using the developed models, even in the absence of direct access to GPU tensor cores. As a test case, we apply the test vectors from [11] to a model custom TC mode with parameters

```
in_format = 'binary16';
out_format = 'binary32';
params.neab = 0;
params.fma = 8;
params.frmode = 'rne';
```

The test vectors from [11], as provided online ⁴, fail to correctly identify the N_{FMA} and conclude that the N_{FMA} must either be 1 or that this feature does not exist. Extra alignment bits are correctly detected, but incorrectly infers the final rounding mode to be RZ instead of RNE. This incorrect conclusion arises mainly because of the absence of extra alignment bits. Therefore, as discussed in [13], the feature

⁴<https://doi.org/10.5281/zenodo.10673370>

targeted tests should be formulated by taking into account n_{eab} to operate correctly.

Next, we change the `neab` to 1 and `frmode='ru'`, round up, while the remaining fields are kept same. Reapplying the test vectors again fails to determine the correct N_{FMA} , suggesting $N_{\text{FMA}} \geq 16$. However, the presence of one extra bit and the use of round up mode are correctly detected. This demonstrates that custom tensor core models can be simulated using the proposed package to validate the robustness of test vectors targeted at detecting features of tensor cores. In addition, it can also be used to determine whether a particular test vector remains invariant to varying other numerical features.

B. Multi-Word Algorithms for Emulating High-Precision GEMM on Tensor Cores

Multi-word arithmetic is a technique of emulating high-precision matrix multiplication with low precision tensor cores. It consists of splitting high-precision input matrices into several low-precision matrices, multiplying them with tensor cores, and adding up the products either in tensor cores or the CUDA cores. In order to demonstrate how one may use the MATLAB tensor core models, we have reproduced the experiments of Mary and Mikaitis [20, Sec. 5] on them.

Figure 7 shows the norm-wise errors, where $\|\cdot\|_{\infty}$ is the infinity norm of a matrix, on five different tensor core models (V100, A100, the H100 which also covers H200 and the B200, L40S, and a custom variant of the B200 which uses round to nearest instead of bit truncation) with the input format set to fp8, fp16 and bf16, and the output format set to fp32. The number of words, which defines how accurate the emulation will be, is shown at the top of each of the sub-figures.

The modified B200 model has rounding to nearest instead of bit truncation—this is applied when an internal accumulator is rounded to the output format, not on the alignments of significands, which are still truncated as in the standard B200 tensor core model.

Interestingly, for single-word arithmetic, all models match up except when the problem size increases close to $n = 10^6$. For double- and triple-word arithmetic, the results show that the V100 tensor core provides two orders of magnitude lower error at $n = 10^6$. This may be caused by B200 tensor core model having more accurate accumulator with $n_{\text{eab}} = 2$, which is rounded to zero, making the error larger than the V100 tensor core’s result. This can occur if the V100 result is above the reference result, whilst the B200 result is closer to the reference, but below it, so that RZ pushes it further below. We have tested this hypothesis by enabling RN in the B200, which demonstrates an improvement. Further analysis of this behavior is out of the scope of this paper and we leave it for future work. Finally, the L40S GPU is, as expected, the least accurate because of the 13 fractional bits in the accumulator as discussed in Section IV-A5.

We expect similar differences in mixed-precision iterative refinement where GEMM operations are executed using different tensor core models [1]. This observation opens up interesting avenues for investigation into how factors such as extra

alignment bits, FMA size, and rounding modes influence the behavior and accuracy of such mixed-precision computations.

The data and the code for producing Fig. 7 is available.⁵

VI. CONCLUSION

We have discussed the research behind the development of the MATLAB Tensor Core v0.1 toolbox. The toolbox contains various NVIDIA GPU tensor core models, as well as a parameterised model that can be used to instantiate variants of real tensor cores for research purposes. The models were verified against the GPU hardware by large-scale randomised testing and model refinement. The proposed toolbox includes tensor core models for NVIDIA A2, A30, A100, Ada 1000 RTX, L40S, H100, H200, and B200, supporting all input precision formats available in CUDA, except binary64. For binary64, NVIDIA GPU tensor cores behave as sequential chains of IEEE-compliant FMAs; therefore, MATLAB’s built-in `fma` function can be used to emulate such tensor core behaviour. In addition to the fixed models, we provide a custom tensor-core model that enables users to simulate arbitrary configurations by adjusting the FMA size, the number of extra bits used for aligning significands, and the rounding mode (supporting RNE, RZ, RD, and RU). For matrix multiplication, the toolbox utilises the MATLAB Parallel Computing Toolbox to create a parallel pool of workers (using the default profile). This dispatches inner products within a GEMM across multiple MATLAB engines.

In the future, this toolbox will be actively maintained through regular versioned releases on GitHub. We plan to improve both the functionality and performance, by porting the back-end to a lower level language, by porting the front-end to other languages such as Python and Julia, and by adding new GPU tensor core and matrix engine models. We also plan to add different GEMM algorithms and improve the validation in Algorithm 1 by exploring different distributions of randomised test vectors and potentially implementing Schryer’s [26] method.

IEEE 754 [8] and P3109 [7] do not standardise reduction operations, such as multi-term addition. We hope that a similar of GPU matrix multiplier models will allow users to understand the differences and how applications may be affected, and impact future standardisation efforts.

VII. ACKNOWLEDGMENT

We thank John Hodrien at University of Leeds for technical support with the AIRE machine containing the NVIDIA L40S and A2, and The COSmology MACHine (COSMA) support at Durham University for providing the access to A30, V100, A100, H100, and H200 GPUs. We also thank Jack Dongarra, John Gunnel, Eduardo Basurto, and Eric Rife for arranging access to the B200 GPUs. Both authors are funded by the EPSRC grant “*Informing Future Numerical Standards by Determining Features of Non-Standard Mathematical Hardware*”, ref. UKRI151.

⁵<https://github.com/north-numerical-computing/MATLAB-tensor-core/tree/main/experiments>

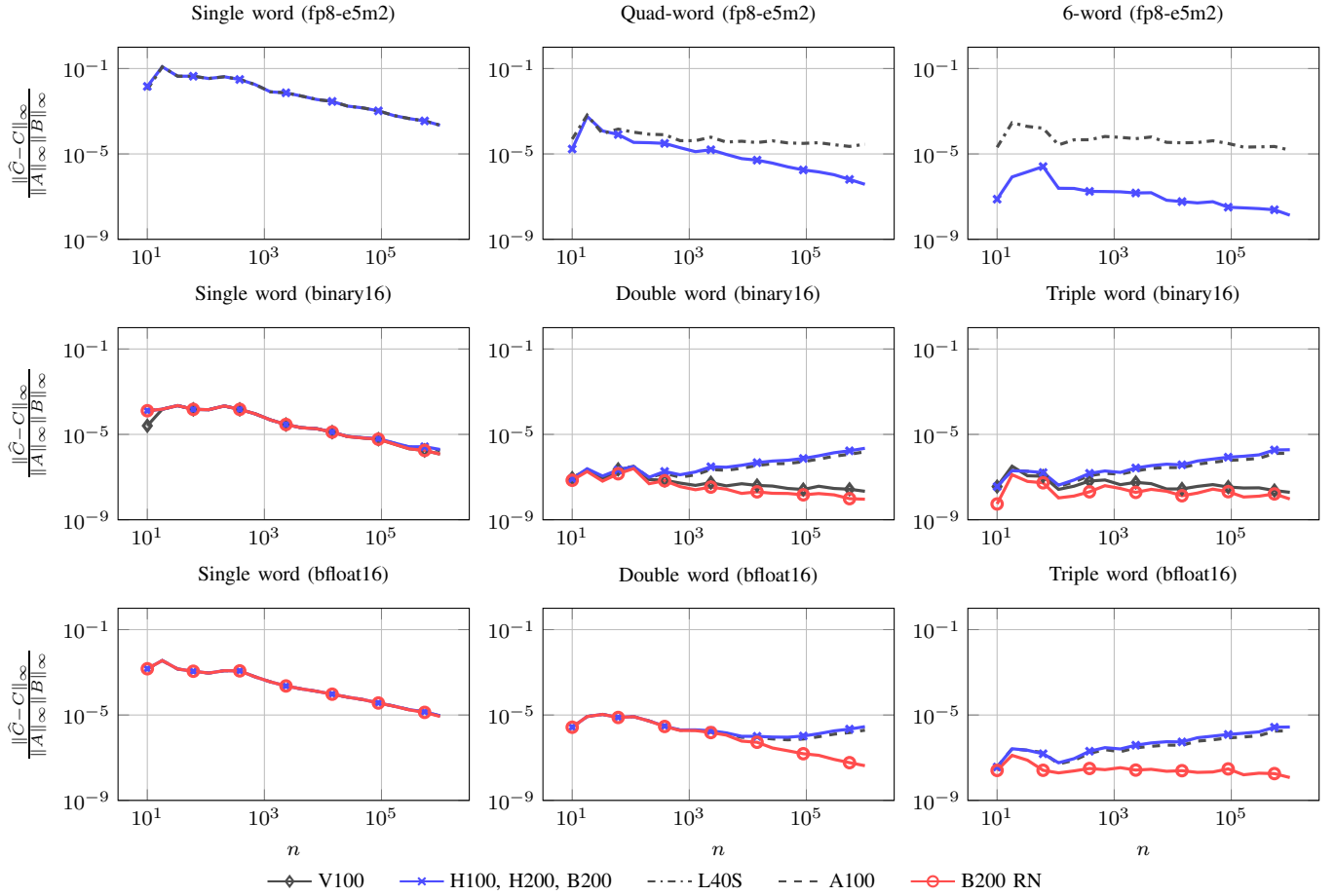


Fig. 7. Multi-word arithmetic experiment presented by Mary and Mikaitis [20, Sec. 5] on the simulation of various tensor cores. We have reproduced the experiment on four different tensor core generations modelled in MATLAB. Relative norm-wise errors of matrix multiplication, compared with a default MATLAB binary64 multiplication, are shown. The input matrices to the GEMM are $A \in \mathbb{R}^{10 \times n}$ and $B \in \mathbb{R}^{n \times 10}$. These matrices are multiplied with a multi-word algorithm [20, Sec. 4] by splitting them into several fp8-e5m2, fp16, or bf16 words.

REFERENCES

- [1] A. Haidar, H. Bayraktar, S. Tomov, J. Dongarra, and N. J. Higham, "Mixed-precision iterative refinement using tensor cores on GPUs to accelerate solution of linear systems," *Proceedings of the Royal Society A: Mathematical, Physical and Engineering Sciences*, vol. 476, no. 2243, p. 20200110, 2020.
- [2] N. J. Higham and T. Mary, "Mixed precision algorithms in numerical linear algebra," *Acta Numerica*, vol. 31, pp. 347–414, May 2022.
- [3] J. Dongarra, J. Gunnels, H. Bayraktar, A. Haidar, and D. Ernst, "Accelerating supercomputing: AI-hardware-driven innovation for speed and efficiency," in *2025 IEEE High Performance Extreme Computing Conference (HPEC)*, 2025, pp. 1–7.
- [4] AMD, "Datasheet: AMD instinct MI355X GPU," 2025. [Online]. Available: <https://www.amd.com/content/dam/amd/en/documents/instinct-tech-docs/product-briefs/amd-instinct-mi355x-gpu-brochure.pdf>
- [5] NVIDIA, "NVIDIA Blackwell architecture technical brief," 2025. [Online]. Available: <https://resources.nvidia.com/en-us-blackwell-architecture>
- [6] P. Micikevicius, S. Oberman, P. Dubey, M. Cornea, A. Rodriguez, I. Bratt, R. Grisenthwaite, N. Jouppi, C. Chou, A. Huffman, M. Schulte, R. Wittig, D. Jani, and S. Deng, "OCP 8-bit floating point specification (OFP8)," Open Compute Project, Tech. Rep., Jun. 2023, revision 1.0. [Online]. Available: <https://www.opencompute.org/documents/ocp-8-bit-floating-point-specification-ofp8-revision-1-0-2023-12-01-pdf-1>
- [7] "Interim report on binary floating-point formats for machine learning," Tech. Rep., Nov. 2025, version 3.2. [Online]. Available: <https://github.com/P3109/Public/blob/main/Shared%20Reports/IEEE%20WG%20P3109%20Interim%20Report%20v3.1.pdf>
- [8] *IEEE Standard for Floating-Point Arithmetic, IEEE Std 754-2019 (revision of IEEE Std 754-2008)*. Piscataway, NJ, USA: Institute of Electrical and Electronics Engineers, Jul. 2019.
- [9] B. Hickmann and D. Bradford, "Experimental analysis of matrix multiplication functional units," in *2019 IEEE 26th Symposium on Computer Arithmetic (ARITH)*, Oct. 2019, pp. 116–119.
- [10] M. Fasi, N. J. Higham, M. Mikaitis, and S. Pranesh, "Numerical behavior of NVIDIA tensor cores," *PeerJ Computer Science*, vol. 7, p. e330, 2021.
- [11] X. Li, A. Li, B. Fang, K. Swirydowicz, I. Laguna, and G. Gopalakrishnan, "FTTN: Feature-targeted testing for numerical properties of NVIDIA & AMD matrix accelerators," in *2024 IEEE 24th International Symposium on Cluster, Cloud and Internet Computing (CCGrid)*, 2024, pp. 39–46.
- [12] B. Valpey, X. Li, S. Pai, and G. Gopalakrishnan, "An SMT formalization of mixed-precision matrix multiplication," in *NASA Formal Methods*. Cham: Springer Nature Switzerland, 2025, pp. 360–379.
- [13] F. A. Khattak and M. Mikaitis, "Generalized methodology for determining numerical features of hardware floating-point matrix multipliers: Part I," in *2025 IEEE High Performance Extreme Computing Conference (HPEC)*, Wakefield, MA, USA, Oct. 2025.
- [14] K. E. Hillesland and A. Lastra, "GPU floating-point Paranoia," in *ACM Workshop on General-Purpose Computing on Graphics Processors (GP²)*. Los Angeles, CA, USA: ACM, Aug. 2004.

- [15] X. Y. Tan, D. Boland, and G. Constantinides, "FPGA Paranoia: Testing numerical properties of FPGA floating point ip-cores," in *Reconfigurable Computing: Architectures, Tools and Applications*, O. C. S. Choy, R. C. C. Cheung, P. Athanas, and K. Sano, Eds. Berlin, Heidelberg: Springer Berlin Heidelberg, 2012, pp. 290–301.
- [16] M. Fasi and M. Mikaitis, "CPFloater: A C library for simulating low-precision arithmetic," *ACM Trans. Math. Softw.*, vol. 49, no. 2, pp. 18:1–18:32, Jun. 2023.
- [17] S. Markidis, S. W. D. Chien, E. Laure, I. B. Peng, and J. S. Vetter, "NVIDIA tensor core programmability, performance & precision," in *Proceedings of the 32nd IEEE International Parallel and Distributed Processing Symposium Workshops*, Vancouver, BC, Canada, Aug. 2018, pp. 522–531.
- [18] L. Pisha and Ł. Ligowski, "Accelerating non-power-of-2 size Fourier transforms with GPU tensor cores," in *Proceedings of the 2021 IEEE International Parallel and Distributed Processing Symposium*, Portland, OR, USA, May 2021, pp. 507–516.
- [19] H. Ootomo and R. Yokota, "Recovering single precision accuracy from tensor cores while surpassing the FP32 theoretical peak performance," *The International Journal of High Performance Computing Applications*, vol. 36, no. 4, pp. 475–491, Jun. 2022.
- [20] T. Mary and M. Mikaitis, "Error analysis of matrix multiplication with narrow range floating-point arithmetic," *SIAM J. Sci. Comput.*, vol. 47, no. 4, pp. B785–B800, 2025.
- [21] M. Mikaitis, "Monotonicity of multi-term floating-point adders," *IEEE Trans. Comput.*, vol. 73, no. 6, pp. 1531–1543, Feb. 2024.
- [22] H. Kaul, M. Anders, S. Mathew, S. Kim, and R. Krishnamurthy, "Optimized fused floating-point many-term dot-product hardware for machine learning accelerators," in *2019 IEEE 26th Symposium on Computer Arithmetic (ARITH)*, 2019, pp. 84–87.
- [23] B. Hickmann, J. Chen, M. Rotzin, A. Yang, M. Urbanski, and S. Avancha, "Intel Nervana Neural Network Processor-T (NNP-T) fused floating point many-term dot product," in *2020 IEEE 27th Symposium on Computer Arithmetic (ARITH)*, 2020, pp. 133–136.
- [24] P. Blanchard, N. J. Higham, F. Lopez, T. Mary, and S. Pranesh, "Mixed precision block fused multiply-add: Error analysis and application to GPU tensor cores," *SIAM Journal on Scientific Computing*, vol. 42, no. 3, pp. C124–C141, 2020.
- [25] A. F. Tenca, "Multi-operand floating-point addition," in *2009 19th IEEE Symposium on Computer Arithmetic*, 2009, pp. 161–168.
- [26] N. L. Schryer, "A test of a computer's floating-point arithmetic unit," AT&T Bell Laboratories, Murray Hill, NJ, Murray Hill, NJ 07974, Technical Report Computer Science Technical Report 89, Feb. 1981.
- [27] NVIDIA, "NVIDIA Tesla V100 GPU architecture," 2017. [Online]. Available: <https://images.nvidia.com/content/volta-architecture/pdf/volta-architecture-whitepaper.pdf>
- [28] Intel Corporation, "BFLOAT16—hardware numerics definition," Available at <https://software.intel.com/en-us/download/bfloat16-hardware-numerics-definition> (accessed 15 July 2020), Nov. 2018, white paper. Document number 338302-001US.